AGU PUBLICATIONS

Geophysical Research Letters

RESEARCH LETTER
10.1002/2016GL068888

Key Points:
- High-resolution rainfall, surface, and groundwater isoscapes computed in a complex tropical mountainous region
- Strong orographic separation of rainfall isotope ratios across the Caribbean and Pacific slopes
- P/GW ratios indicate groundwater recharge controlled by preferential flow (Caribbean slope) and slower soil matrix flow (Pacific slope)

Supporting Information:
- Supporting Information S1
- Data Set S1
- Data Set S2
- Data Set S3

Correspondence to:
R. Sánchez-Murillo,
ricardo.sanchez.murillo@una.cr

Citation:
Sánchez-Murillo, R., and C. Birkel (2016), Groundwater recharge mechanisms inferred from isoscapes in a complex tropical mountainous region, *Geophys. Res. Lett.*, *43*, 5060–5069, doi:10.1002/2016GL068888.

Received 29 JAN 2016
Accepted 6 MAY 2016
Accepted article online 11 MAY 2016
Published online 23 MAY 2016

Groundwater recharge mechanisms inferred from isoscapes in a complex tropical mountainous region

Ricardo Sánchez-Murillo[1] and Christian Birkel[2,3]

[1]Stable Isotope Research Group, National University of Costa Rica, Heredia, Costa Rica, [2]Department of Geography, University of Costa Rica, San José, Costa Rica, [3]Northern Rivers Institute, University of Aberdeen, Aberdeen, Scotland

Abstract Stable isotope variations and groundwater recharge mechanisms remain poorly understood across the tropics, particularly in Central America. Here stable isotopes ($\delta^{18}O$ and $\delta^{2}H$) in groundwater, surface water, and rainfall are used to produce high-resolution (100 m^2 grid) isoscapes for Costa Rica, from which an isotope ratio of precipitation to groundwater (P/GW) is estimated to elucidate the dominant groundwater recharge processes. Spatially, groundwater and surface water isotope ratios depict the strong orographic separation into the Caribbean and Pacific slopes induced by moisture transport directly from the Caribbean Sea and the eastern tropical Pacific Ocean. P/GW isotope ratios reveal that groundwater recharge is biased toward intensive and more depleted monthly rainfall across the Pacific slope with clear evidence of secondary evaporation indicating slower soil matrix recharge processes. On the other hand, P/GW isotope ratios indicate a weak influence of secondary evaporation across the Caribbean slope suggesting rapid recharge via preferential flow paths.

1. Introduction

The use of isoscapes has become a valuable tool to understand hydro-climatic processes from regional or nationwide scales [*Kendall and Coplen,* 2001; *Bowen et al*., 2007; *Wassenaar et al*., 2009; *West et al*., 2014] to global perspectives [*Bowen and Wilkinson*, 2002; *Bowen and Revenaugh*, 2003; *Terzer et al*., 2013; *Jasechko et al*., 2013; *Evaristo et al*., 2015; *Good et al*., 2015]. The increased use of stable isotopes in hydrology relies on the development of inexpensive instrumentation based on laser spectroscopy which has enhanced the ability to achieve greater temporal and spatial resolution [*Gupta et al*., 2009; *Good et al*., 2014; *Munksgaard et al*., 2015]. In the tropics, where long-term hydrologic and climatic records are limited or inexistent, isoscapes emerge as a low-cost and effective tracer technique to understand precipitation dynamics [*Lachniet and Paterson,* 2009; *Moerman et al*., 2013; *Sánchez-Murillo et al.*, 2016], groundwater recharge mechanisms [*Heilweil et al*., 2009; *Moerman et al*., 2014; *Baraer et al*., 2015; *Jasechko and Taylor,* 2015], reconstruct past climate [*Vimeux et al*., 2005; *Lachniet,* 2009; *Risi et al*., 2010], and ultimately, enhance water resources management in developing countries using isoscapes as a physically based planning tool [*Bowen and Good,* 2015]. However, to be able to use isoscapes as a management tool, the spatial resolution needs to be improved and adapted to regional and local scales, which invoke more sampling efforts to capture spatiotemporal variations, particularly in mountainous landscapes due to their inherent environmental complexity [*Yamanaka et al*., 2015].

Central America is home to ~47 million inhabitants and highly depends on groundwater extraction ($1.9 \times 10^4\ m^3 yr^{-1}$) as a primary water resource due to the decline in quality and quantity of surface water sources [*Ballestero et al*., 2007]. In addition, limited high-resolution and grid-based information is available regarding precipitation, recharge, discharge, and evapotranspiration rates. In this region, during the last 100 years, average surface temperature has increased by 0.5 to 1.0°C and the number of warm days (% of days when maximum daily temperature >90th) has risen by about 2.5% each decade since 1970s [*Aguilar et al*., 2005; *Knutson et al*., 2006], turning the region into the most prominent tropical hot spot under future climate change scenarios [*Giorgi*, 2006]. The increasing trend for long-term droughts [*Sheffield and Wood*, 2008] poses a challenge for truly integrated water resources management [*McDonnell*, 2008; *Giordano and Shah*, 2014; *Foster and MacDonald*, 2014; *Vrba and Renaud*, 2015], particularly in the light of absent national water balances.

In this study, stable isotope ($\delta^{18}O$ and $\delta^{2}H$) archives in groundwater, surface water, and precipitation are combined with new stable isotope data from exhaustive sampling campaigns to produce high-resolution

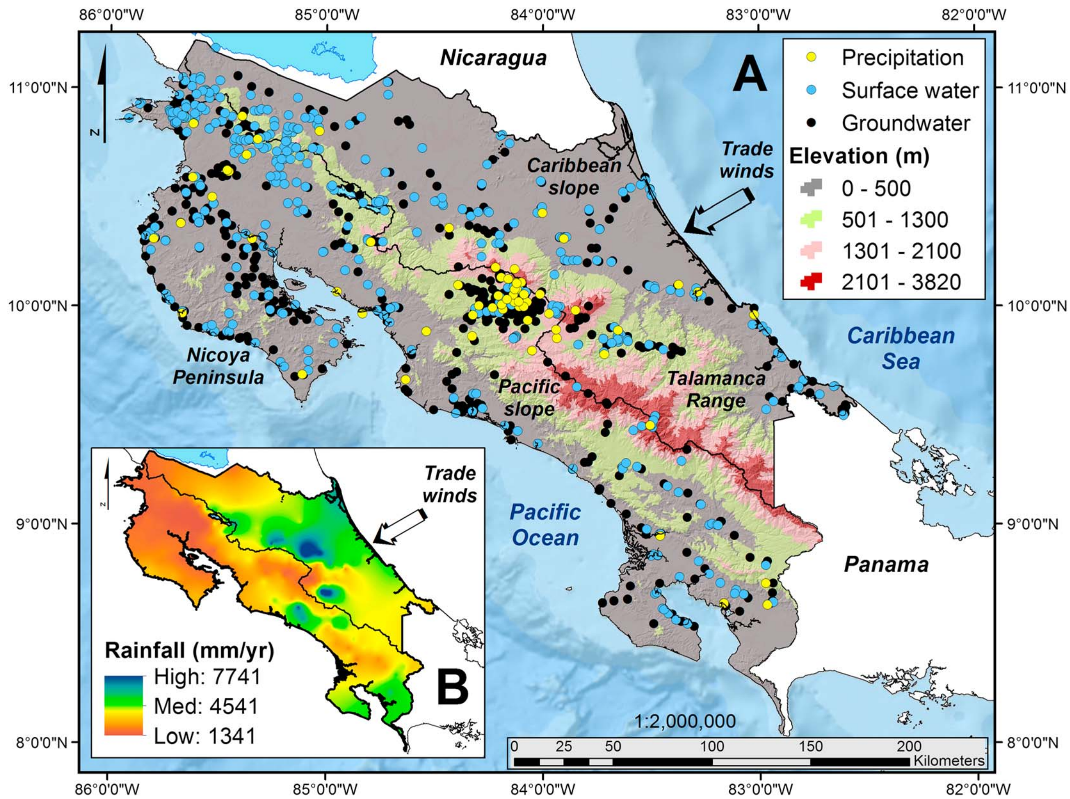

Figure 1. (a) Map of the study area including precipitation (yellow dots), groundwater (black dots), and surface water (blue dots) sampling locations. The elevation range is color coded. The black line crossing from NW to SE indicates the continental divide boundary between the Pacific and Caribbean slopes. The prevailing trade winds direction (NE → SW) is represented by a white-black arrow. (b) The inset shows the spatial distribution of mean annual precipitation (MAP) in mm/yr.

isoscapes (100 m^2 grid) for Costa Rica. These isoscapes are coupled with new actual evapotranspiration and discharge rates to provide spatial and physically based understanding of recharge processes across a complex tropical mountainous region. The isotope and geospatial approach presented in this study may be translated to other tropical regions where groundwater vulnerability [*Vrba and Richts*, 2015] due to climate variability and limited water resources planification poses the potential for disruption of ecological assemblages and socioeconomic activities.

2. Climate Generalities of Costa Rica

Costa Rica is located on the Central America Isthmus between 8° and 12°N latitude and 82° and 86°W longitude (Figure 1a). Four regional air circulation processes predominantly control the climate of Costa Rica: NE trade winds, the latitudinal migration of the Intertropical Convergence Zone (ITCZ), cold continental outbreaks, and sporadic influence of Caribbean cyclones [*Waylen et al.*, 1996; *Sáenz and Durán-Quesada*, 2015]. These circulation processes produce two predominant rainfall maxima, one in May and June and the second one in August-September-October (ASO), which are interrupted by a relative minimum in July known as the Mid-Summer Drought (MSD) [*Magaña et al.*, 1999; *Maldonado et al.*, 2013]. In addition to these circulation processes, the continental divide (i.e., a mountainous range that extends from NW to SE with a maximum elevation at the Chirripó peak: 3,820 m above sea level (asl)) also influences precipitation patterns across the country, dividing the territory into the Caribbean and Pacific slopes. In general, annual precipitation in Costa Rica varies from <1500 mm in the drier northwestern region, ~2500 mm in the Central Valley, and up to ~7000 mm on the Caribbean side of the Talamanca range (Figure 1b). Temperature seasonality is low throughout the country (<2°C). The mean annual temperature on the coastal lowlands is about 27°C, 20°C in the Central Valley at around 1100 m asl, and below 10°C at the summits of the Talamanca range.

3. Data Sources and Methods

3.1. Stable Isotope Archives

Stable isotope archives of precipitation ($N = 679$; monthly composite samples) were obtained from the Global Network of Isotopes in Precipitation also known as GNIP [*International Atomic Energy Agency/World Meteorological Organization*, 2015]. This data set is composed of three relatively short-term sampling campaigns (monthly samples): 1990–1992, 1997–1998, and 2002–2005; a detailed description of this data set for Costa Rica is presented in *Sánchez-Murillo et al.* [2013]. Stable isotope archives of groundwater ($N = 752$; sampling period: 1982–2009) and surface waters ($N = 470$; sampling period: 1982–2009) were obtained directly from the Water Resources Programme of the International Atomic Energy Agency.

3.2. Recent Stable Isotope Data

3.2.1. Precipitation

New stable isotope data of precipitation is composed of daily ($N = 1{,}208$; sampling period: 2012–2015) and weekly ($N = 947$; sampling period: 2013–2015) samples across 19 stations in Costa Rica. Daily rainfall was conducted using a passive collector (Palmex Ltd., Zagreb, Croatia) [*Gröning et al.*, 2012], while weekly samples were collected using a traditional mineral oil-based collector [*International Atomic Energy Agency (IAEA)*, 2012]. The large sample volume, often collected over weekly intervals (>1.5 L), facilitated the separation process, providing oil-free water samples for isotope analysis. Average annual amount-weighted ratios [*Dansgaard*, 1964] were calculated to consolidate a single data set with the GNIP archives. The ongoing isotope monitoring network in precipitation provides a better spatial distribution across different climatic zones, altitudes, and biomes of Costa Rica which are representative of similar conditions across Central America.

3.2.2. Surface Water and Groundwater

Similarly, the novel stable isotope dataset is composed of groundwater ($N = 295$) and surface waters ($N = 485$) sampled targeting base flow conditions. Since base flow is described as the cumulative outflow from all upstream riparian aquifers during rainless periods [*Brutsaert*, 2005], precipitation records in each sampling region were carefully revised (prior and after) to ensure sample collection was conducted as far as possible without recent precipitation in the area (>7 days). In addition, base flow recession in the tropics mostly occurs from hours to 1–2 days [*Peña-Arancibia et al.*, 2010] which facilitated the discrimination of sampling periods during base flow. The main goal of the recent sampling campaigns (2013–2015) was to obtain high spatial resolution and country-wide coverage for the construction of interpolated isoscapes. Groundwater samples were collected from automated drinking water wells. Well valves were opened and the water flowed for 10 min prior to sample collection to avoid stagnant water, in case the well was turned off for long time according to local well operators. Surface waters were exclusively collected at the flowing sections of streams to avoid stagnant ponds with strong evaporative signals. Both groundwater and surface water samples were collected in 30 mL glass E-C borosilicate bottles with tetrafluoroethylene (TFE)-lined caps (Wheaton Science Products, USA). Bottles were filled with no head space, covered with parafilm (Thermo Scientific, USA) avoiding exchange with atmospheric moisture, and stored upside down at 5°C until analysis.

3.2.3. Stable Isotope Analysis

Stable isotope analyses were conducted at the Stable Isotope Research Group facilities of the National University (Heredia, Costa Rica) using a Cavity Ring Down Spectroscopy (CRDS) water isotope analyzer L2120-*i* (Picarro, USA). The secondary standards were as follows: Moscow Tap Water, MTW ($\delta^2H = -131.4$‰, $\delta^{18}O = -17.0$‰), Deep Ocean Water, DOW ($\delta^2H = -1.7$‰, $\delta^{18}O = -0.2$‰), and Commercial Bottled Water, CAS ($\delta^2H = -64.3$‰, $\delta^{18}O = -8.3$‰). MTW and DOW standards were used to normalize the results to the VSMOW2-SLAP2 scale, while CAS was used as a quality control and drift control standard. The analytical long-term precision was ± 0.5‰ (1σ) for δ^2H and ± 0.1‰ (1σ) for $\delta^{18}O$.

3.3. Geospatial Analysis of Isotopes and Hydrological Fluxes

All raster isoscapes and hydrological maps were developed using a 100 m^2 grid resolution. Interpolations were performed in ArcGIS 10.3 (ESRI, USA) based on a thin plate spline algorithm [*Franke*, 1982]. Spatial errors were assessed using a "leave-one-out" cross validation procedure [*Shao*, 1993] from which the mean residuals (MSE) in ‰ and millimeter were calculated. The precipitation isoscape was calculated using amount-weighted isotope ratios [*Dansgaard*, 1964], while the groundwater and surface water isoscapes were constructed using mean annual values. We further calculated a precipitation to groundwater (P/GW) $\delta^{18}O$ ratio to assess spatial patterns of groundwater recharge similar to *Jasechko and Taylor* [2015]. Due to the linear

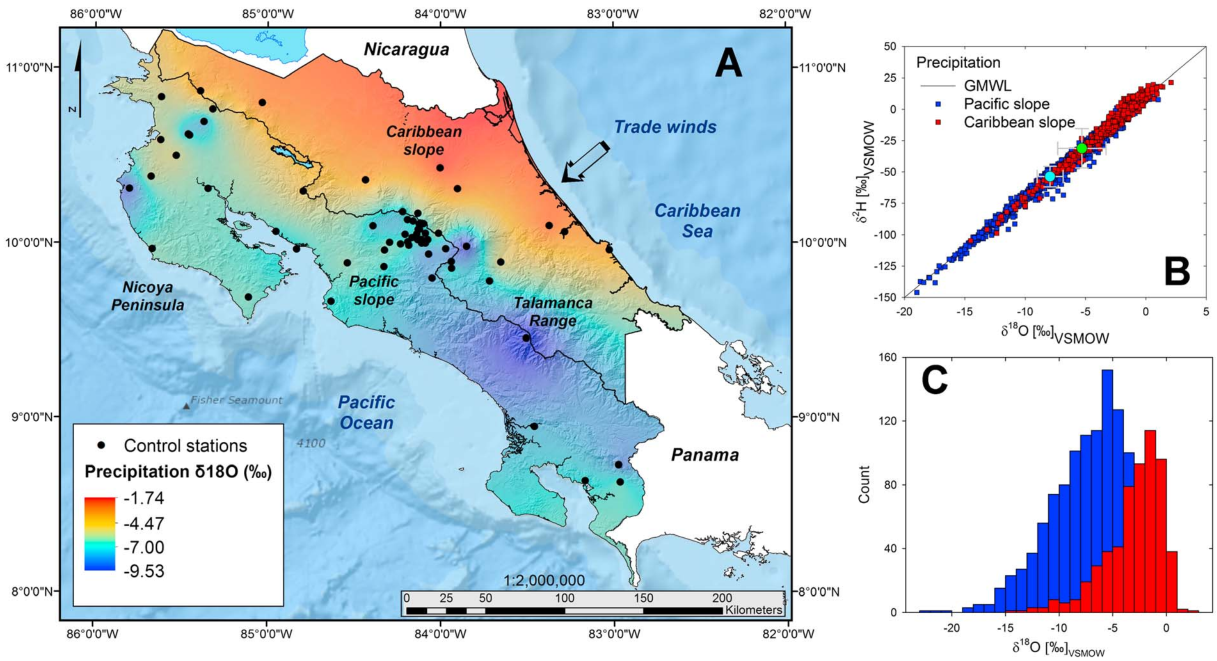

Figure 2. (a) Interpolated precipitation isoscape of $\delta^{18}O$ (‰) for Costa Rica. The black dots represent the sampling locations. (b) Linear relationship between $\delta^{2}H$ and $\delta^{18}O$ for both slopes. The green and light blue dots in Figure 2b represent the mean groundwater isotope composition within the Caribbean and Pacific slopes for comparison purposes, respectively. The grey error bars explain the lager variability found on the Caribbean slope compared to the smaller range across the Pacific slope. (c) The histogram shows the distribution of $\delta^{18}O$ per slope. Pacific and Caribbean samples are denoted by blue and red color, respectively.

relationship between $\delta^{18}O$ and $\delta^{2}H$, only $\delta^{18}O$ was selected to estimate P/GW isotope ratios. In addition to the isoscape analysis, high-resolution and grid-based hydrological variables were determined to complement the understanding of groundwater recharge processes. Long-term mean annual precipitation (MAP, mm/yr) data were compiled using 276 stations with at least 10 years of continuous record, where >80% falls in the period from 1960 to 2000. Mean annual actual evapotranspiration (AET, mm/yr) was derived from monthly Moderate Resolution Imaging Spectroradiometer (MODIS) products for the period from 2000 to 2013 [*Moderate Resolution Imaging Spectroradiometer*, 2014]; the final MODIS product used a nearest neighbor interpolation to fill in gaps and to create a smooth and continuous surface between any transition of different land uses prior to conversion into mm/yr. The mean annual runoff (MAR, mm/yr) was calculated using a simple water balance difference assuming negligible storage changes.

4. Isotopic Patterns Across a Complex Tropical Mountainous Region

The presence of a mountainous range that extends from the NW to the SE divides the territory into the Caribbean and Pacific slopes (Figure 1a), influencing the precipitation regimes in time and magnitude across the country (MAP = 3,085 ± 994 mm/yr) (Figure 1b and Figures S1a and S1b in the supporting information). Overall, across the Caribbean slope $\delta^{18}O$ averaged −5.0 ± 2.4‰ (rainfall), −5.3 ± 2.0‰ (groundwater), and −5.6 ± 2.1‰ (surface water), while throughout the Pacific slope $\delta^{18}O$ averaged −7.0 ± 1.0‰ (rainfall), −7.9 ± 1.1‰ (groundwater), and −7.2 ± 2.1‰ (surface water). The well-known isotopic altitude effect [*Clark and Fritz*, 1997] coupled with the prevailing trade winds direction (NE → SW) [*Sánchez-Murillo et al.*, 2016] produces strong spatial variations in Central America. For $\delta^{18}O$ in rainfall, the altitude effect across the country averaged −1.4‰ per 1 km for stations above ~340 m of elevation ($r^2 = 0.43$, $P < 0.001$). Furthermore, this inverse altitude effect is stronger within the Caribbean slope than the Pacific slope; a similar trend has been reported by *Lachniet et al.* [2007] in Panama and *Wassenaar et al.* [2009] in Mexico. The stronger rainout effect observed over the Caribbean slope is most likely related to the direct influence of the trade winds and nearby moisture transport from the Caribbean Sea, whereas in the Pacific slope the combination of the rain shadow effect, more complex topography, and deep convective activity throughout ASO results in a weaker elevation trend. Therefore, the isotopic variability within the Pacific slope is likely biased toward the precipitation amount effect (Figures 2a and 2b).

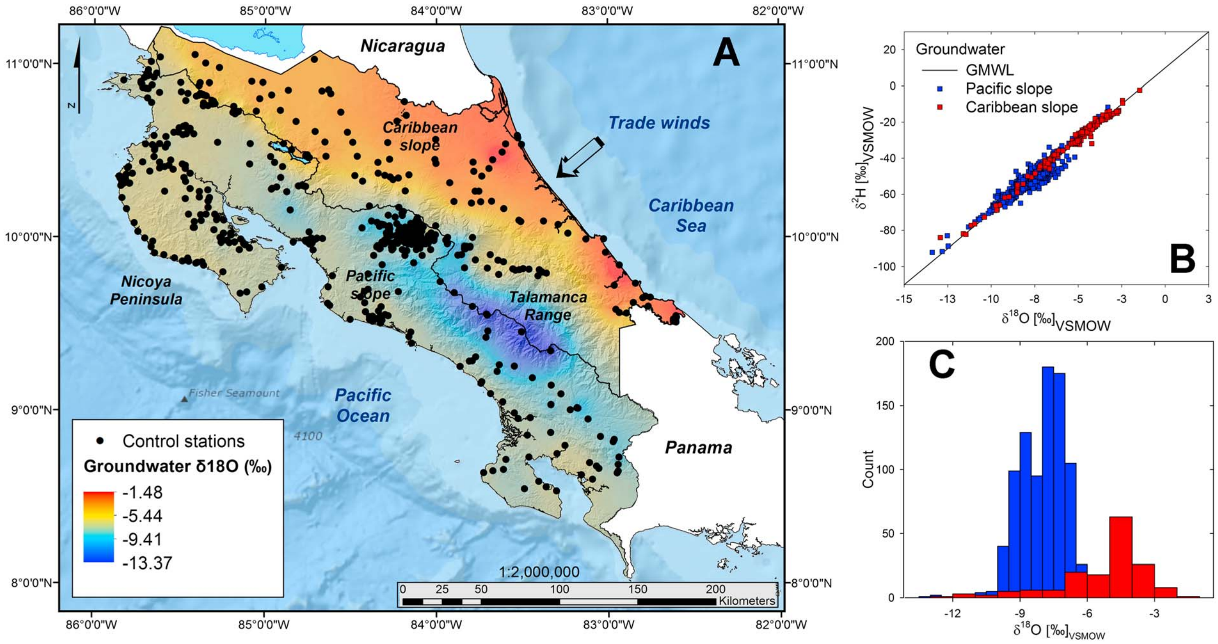

Figure 3. (a) Interpolated groundwater isoscape of δ^{18}O (‰) for Costa Rica. The black dots represent the sampling locations. (b) Linear relationship between δ^2H and δ^{18}O for both slopes. (c) The histogram shows the distribution of δ^{18}O per slope. Pacific and Caribbean samples are denoted by blue and red color, respectively.

For groundwater, the inverse δ^{18}O correlation with altitude was -0.74‰ per 1 km ($r^2 = 0.20$, $P < 0.001$) within the Pacific slope and -2.5‰ per 1 km ($r^2 = 0.77$, $P < 0.001$) in the Caribbean slope (Figure 3a). For surface water, the inverse δ^{18}O correlation with altitude was -1.4‰ per 1 km ($r^2 = 0.26$, $P < 0.001$) within the Pacific slope and -2.6‰ per 1 km ($r^2 = 0.60$, $P < 0.001$) in the Caribbean slope (Figure 4a).

The linear relationship between δ^2H and δ^{18}O in groundwater and surface waters are used as indicators of secondary evaporation. In evaporating surface water and groundwater, the δ^2H and δ^{18}O ratios, are shifted

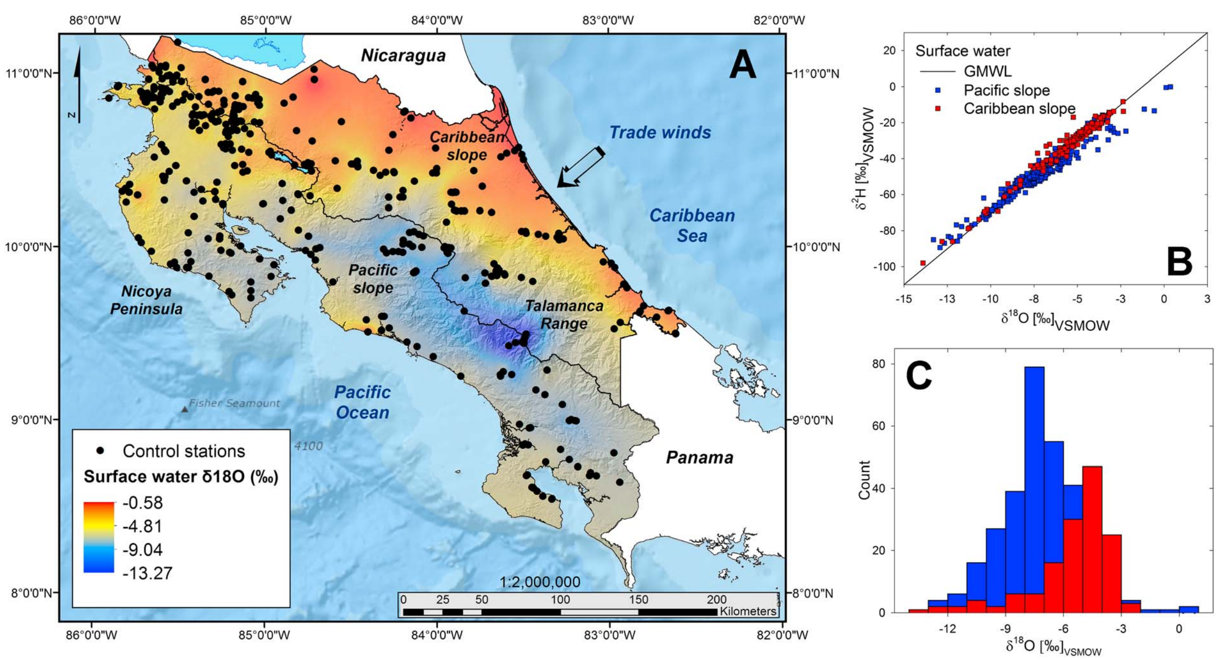

Figure 4. (a) Interpolated surface water isoscape of δ^{18}O (‰) for Costa Rica. The black dots represent the sampling locations. (b) Linear relationship between δ^2H and δ^{18}O for both slopes. (c) The histogram shows the distribution of δ^{18}O per slope. Pacific and Caribbean samples are denoted by blue and red color, respectively.

to more enriched values along evaporation lines with slopes and intercepts considerably smaller than 8 and 10, respectively [*Mook*, 2006]. In the Caribbean slope, the Caribbean slope, the linear relationships between δ^2H and δ^{18}O for groundwater ($\delta^2H = 7.7\delta^{18}O + 9.6$, $r^2 = 0.99$, $P < 0.001$) and surface water ($\delta^2H = 7.5\delta^{18}O + 9.4$, $r^2 = 0.99$, $P < 0.001$), clearly indicate minimum influence of secondary evaporation enrichment, as a result of rapid infiltration processes via preferential pathways such as soil macropores (i.e., large soil pores that drain freely by gravity and conduct large volumes of water) [*Taylor et al*., 2015] and the relatively high humidity conditions across the Caribbean slope (Figures S2a and S2b). High relative humidity commonly >70% throughout the year and large vegetation coverage implies high transpiration rates across the Caribbean slope (AET ~ 1397–1940 mm/yr, Figure S3). Therefore, Caribbean watersheds are often energy limited since MAP can reach up to 7741 mm/yr. On the contrary, across the Pacific slope, the isotope ratios in surface water and groundwater indicate stronger secondary evaporation, implying a slower soil matrix controlled recharge that allows a greater soil-water attenuation [*Leibundgut et al*., 2009], which is clearly depicted by their respective linear departures along evaporation lines: $\delta^2H = 7.2\delta^{18}O + 3.0$, $r^2 = 0.88$, $P < 0.001$ (groundwater) and $\delta^2H = 6.8\delta^{18}O + 0.9$, $r^2 = 0.95$, $P < 0.001$ (surface water) (Figures 3b and 4b). Remarkably, the meteoric water lines for the Caribbean ($\delta^2H = 8.3\delta^{18}O + 11.2$, $r^2 = 0.98$, $P < 0.001$) and Pacific ($\delta^2H = 8.0\delta^{18}O + 9.3$, $r^2 = 0.98$, $P < 0.001$) slopes are close to the Global Meteoric Water Line relationship ($\delta^2H = 8\delta^{18}O + 10$) [*Craig*, 1961]. Therefore, the isotopic patterns observed both in groundwater and surface water are linked to the recharge-discharge recession characteristics within each slope, which are controlled by climate and soil characteristics [*Brutsaert*, 2005]. For instance, the Caribbean lowlands exhibited the maximum discharge values (MAR ~ 6489 mm/yr, Figure S4), which can be attributed to a displacement process in which rainfall induces the movement of subsurface stored water [*Sophocleous*, 2002]. On the other hand, the Pacific lowland watersheds are often water limited with low MAP (<1500 mm/yr, Figure 2b) and AET (312 mm/yr, Figure S3) rates, areas under water stress with low discharge during the dry season (Figure S4), and relatively high temperatures (>30°C) and low relative humidity values (30–40%), which may enhance secondary evaporation (Figures S2a and S2b).

Since Central America shares a common geomorphologic past [*Coates and Obando*, 1996], represented by the existent NW-SE cordillera that divides the region into the Caribbean and Pacific slopes with similar precipitation regimes [*Alfaro*, 2002] and soil characteristics, it can be expected that groundwater recharge processes may be controlled by similar mechanisms, which enforce the idea of using isoscapes as a reliable regional isotope approach to elucidate dominant hydrological processes. An example of climate and geomorphologic similarity is the "Dry Corridor of Central America," an area that extends from Chiapas, Mexico to northwestern Costa Rica (in the Pacific slope), and also includes Panama's "Arco Seco" dry area; this region has strongly been affected by the recent El Niño event resulting in unified adaptation strategies regarding groundwater extraction for agriculture [*Food and Agriculture Organization of the United Nations*, 2015].

5. Isoscapes and Groundwater Recharge Processes

A clear isotopic separation in rainfall ratios is observed across the Pacific and Caribbean slopes (ranging from −1.9‰ to −10.1‰ δ^{18}O, respectively), which can be explained by the prevailing trade winds direction (NE → SW) [*Sánchez-Murillo et al*., 2016], moisture sources and resulting precipitation regimes, and the elevation gradient. Regarding the moisture transport processes, Central America is affected by the direct influence of evaporative fluxes from the Caribbean Sea and the eastern tropical Pacific Ocean. The semiclosed basin of the Caribbean Sea ($\delta^2H = -75.0$‰ and $\delta^{18}O = -10.6$‰, derived from *Good et al*. [2015]) has a more enriched marine isotope vapor ratio than the eastern tropical Pacific Ocean ($\delta^2H = -100.0$‰ and $\delta^{18}O = -13.75$‰, derived from *Good et al*. [2015]) with an overall difference of −25‰ (δ^2H) and −3.2‰ (δ^{18}O). Similarly, δ^{18}O ratios in seawater across the Central America region show a relative difference of ~1–2‰ between the Caribbean Sea and the eastern tropical Pacific Ocean [*Legrande and Schmidt*, 2006]. These dissimilarities are well depicted in the precipitation isoscape of Costa Rica (Figures 2a and 2b), where the most enriched values occurred on the Caribbean lowlands, while the most depleted values lie along the interior mountain range and along the Pacific coast. The weakening of the trade winds from May to November allows the entering of Pacific moisture resulting in intense convective rainfall during May and June and throughout ASO [*Maldonado et al*., 2013] with depleted isotopic values, whereas from December to April the trade winds present their maximum velocities proving intense monthly rainfall and near-uniformly enriched isotope values

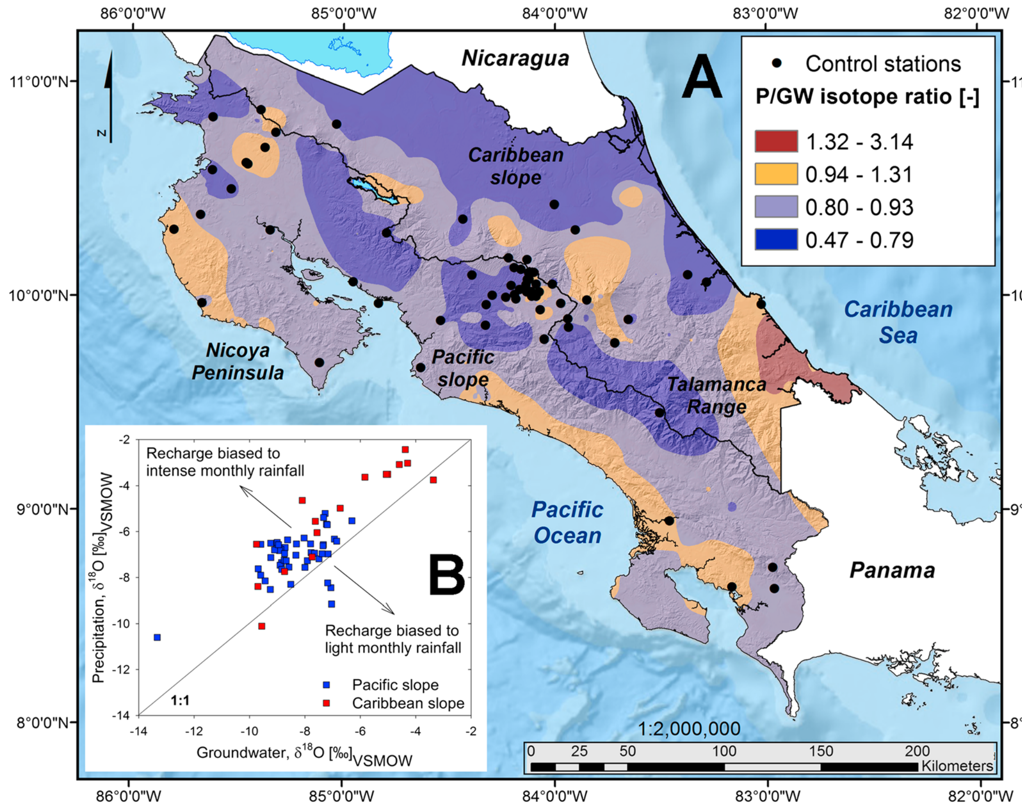

Figure 5. (a) Spatial classification of precipitation to groundwater (P/GW) $\delta^{18}O$ ratios (−) for Costa Rica. The black dots represent the control precipitation locations. (b) The inset shows the relationship between precipitation and groundwater $\delta^{18}O$ ratios (48 stations) following *Jasechko and Taylor* [2015].

across the Caribbean lowlands (Figure S1A). Figure S5a shows the spatial distribution of $\delta^{18}O$ MSE in precipitation and the elevation spectrum of monitoring stations across the Pacific and Caribbean slopes (Figure S5b and S5c). MSE ranged from +2.10 (‰) within the Caribbean lowlands up to −4.16 (‰) at the highest elevation of the Talamanca range. Furthermore, the greater MSE across the Talamanca range emphasizes the need for better monitoring efforts in high-relief tropical mountainous regions [*West et al.*, 2014; *Yamanaka et al.*, 2015] in order to improve global water cycle flux estimations that are often derived from isotopic data with consistent monitoring gaps across remote and complex mountainous regions.

The spatial distribution of $\delta^{18}O$ in meteoric water is reflected by the groundwater isoscape of Costa Rica (Figure 3a). Enriched $\delta^{18}O$ values (−1.5‰) are also present within the Caribbean lowlands, and some intrusion of Caribbean-isotope type signal is observed across topographical depressions (i.e., trade wind passes) along the continental divide. The most negative $\delta^{18}O$ ratios (−13.4‰) occurred across the Talamanca range and intermediate $\delta^{18}O$ compositions (−7.8‰) are presented across the Nicoya Peninsula and NW region of the country. An analogous spatial distribution of $\delta^{18}O$ values is shown in the surface water isoscape (Figure 4a). Groundwater and surface water isotope ratios appear largely unaffected by secondary evaporation within the Caribbean lowlands contrary to the clear evaporation effect across the Pacific slope.

Most importantly, these observed isotope patterns through the hydrological cycle can be used to improve the understanding of key geophysical processes controlling groundwater recharge dynamics in complex tropical mountainous regions. A direct $\delta^{18}O$ comparison of local rainfall to groundwater reveals that (Figures 5a and 5b) 44 out of 48 rainfall stations exhibited groundwater recharge biased toward intense and more depleted monthly rainfall.

Jasechko and Taylor [2015] estimated a global precipitation threshold intensity (under primarily humid conditions and distinct geological settings) producing significant groundwater recharge in the tropics at ~100–300 mm/month. In the Central America region, *Jasechko and Taylor* [2015], reported a threshold intensity decile (>90th) of ~400 mm/month at the Chipilapa-Ahuachapin volcanic aquifer, El Salvador (Pacific slope). Based on this isotope-derived threshold intensity for the pacific region of Central America, groundwater recharge across the Pacific slope is mainly favored during September and October where long-term monthly rainfall exceeds 400 mm/month (Figure S1b), whereas groundwater recharge is more uniformly distributed throughout the year across the Caribbean lowlands between the pantropical threshold intensity of 100 and 300 mm/month. The interpolated P/GW isotope ratios (Figure 5a) show areas where P/GW > 1, which indicates a significant soil matrix-water attenuation in the unsaturated zone and potentially implies shallow groundwater reservoirs, particularly across coastal aquifers within the Pacific slope and the Talamanca lowlands (Figure 5a). Areas relying on high-altitude recharge and/or potentially influenced by interbasin groundwater flow mixing [*Genereux and Jordan*, 2006] with depleted waters are represented by P/GW < 1. The latter areas are mainly located across the high-altitude interior such as the central mountainous range, which provides groundwater resources to over half of Costa Rica's population [*Salguero-Arias et al*., 2006]. The spatial pattern of P/GW isotope ratios that increase from the cordillera down to the coast are most prominent in the Central Pacific region and support the notion of groundwater that is mainly recharged at higher altitudes. P/GW isotope ratios close to 1 are an indication of rapid groundwater recharge often observed across the Caribbean lowlands.

6. Conclusions

This first isotopic synthesis in precipitation, surface water, and groundwater shows that Costa Rica can be separated into two distinct isotopic slopes: more enriched values are commonly observed across the Caribbean lowlands, and depleted isotopic patterns are present within the Pacific highlands and coastal areas. Overall, the Caribbean slope is unaffected by evaporation and generally reflects the influence of direct moisture transport from the Caribbean Sea, whereas a clear secondary evaporation effect is observed across the Pacific slope. P/GW isotope ratios suggest two distinct recharge mechanisms: rapid recharge via preferential flow paths within the Caribbean lowlands and a soil matrix controlled recharge process across the Pacific slope. Pacific recharge is favored during September and October, whereas groundwater recharge is more uniformly distributed throughout the year across the Caribbean lowlands. A first attempt of a high-resolution (100 m^2 grid) nationwide water balance highlighted areas with significant spatial variability of hydrological fluxes which invoke better hydrological monitoring efforts by governmental agencies in order to produce and apply effective water resources plans that can take into account groundwater resilience under current climate change (decadal) and impacts from climate "shocks" (interannual) with particular interest on those areas within the "Dry Corridor of Central America" during El Niño years.

Acknowledgments
This project was supported by International Atomic Energy Agency grant CRP-19747 to R.S.M. under the initiative "Stable isotopes in precipitation and paleoclimatic archives in tropical areas to improve regional hydrological and climatic impact models." The authors would also thank various helping hands that contribute with precipitation, groundwater, and surface water sample collection. C.B. was supported by the University of Costa Rica under project 217-B4-239. We also thank the Programme on Water Resources of the International Atomic Energy Agency for granting access to stable isotope archives of groundwater and surface water in Costa Rica. Gridded water balance products are also available upon request from Christian Birkel (c.birkel@abdn.ac.uk) and Ricardo Sánchez-Murillo (ricardo.sanchez.murillo@una.cr).

References

Aguilar, E., et al. (2005), Changes in precipitation and temperature extremes in Central America and northern South America, 1961–2003, *J. Geophys. Res.*, *110*, D23107, doi:10.1029/2005JD006119.
Alfaro, E. (2002), Some characteristics of the annual precipitation cycle in Central America and their relationships with its surroundings tropical oceans, *Topic. Meteorol. Oceanogr.*, *9*(2), 88–103.
Ballestero, M., V. Reyes, and Y. Astorga (2007), Groundwater in Central America: Its importance, development, and use, with particular reference to its role in irrigated agriculture, in *The Agricultural Revolution: Opportunities and Threats to Development*, CAB International, Wallingford.
Baraer, M., J. McKenzie, B. G. Mark, R. Gordon, J. Bury, T. Condom, J. Gomez, S. Knox, and S. K. Fortner (2015), Contribution of groundwater to the outflow from ungauged glacierized catchments: A multi-site study in the tropical Cordillera Blanca, Peru, *Hydrol. Processes*, *29*(11), 2561–2581, doi:10.1002/hyp.10386.
Bowen G., and Revenaugh J. (2003), Interpolating the isotopic composition of modern meteoric precipitation, *Water Resour. Res.*, *39*(10), 1299, doi:10.1029/2003WR002086.
Bowen, G., and B. Wilkinson (2002), Spatial distribution of δ18O in meteoric precipitation, *Geology*, *30*(4), 315–318, doi:10.1130/0091-7613(2002)030<0315:SDOOIM>2.0.CO;2.
Bowen, G. J., and S. P. Good (2015), Incorporating water isoscapes in hydrological and water resource investigations, *Wiley Interdiscip. Rev.*, *2*(2), 107–119, doi:10.1002/wat2.1069.
Bowen, G. J., Ehleringer, J. R., Chesson, L. A., Stange, E., and Cerling, T. E. (2007), Stable isotope ratios of tap water in the contiguous United States, *Water Resour. Res.*, *43*, W03419, doi:10.1029/2006WR005186.
Brutsaert, W. (2005), *Hydrology: An Introduction*, 605 pp., Cambridge Univ. Press, Cambridge, U. K.
Clark, I. D., and P. Fritz (1997), *Environmental Isotopes in Hydrogeology*, 328 pp., Lewis Publishers, New York.
Coates, A. G., and J. A. Obando (1996), The geologic evolution of the Central American Isthmus, in *Evolution and Environment in Tropical America*, pp. 21–56, Univ. of Chicago Press, Chicago, Ill.
Craig, H. (1961), Isotopic variations in meteoric waters, *Science*, *133*(3465), 1702–1703, doi:10.1126/science.133.3465.1702.
Dansgaard, W. (1964), Stable isotopes in precipitation, *Tellus*, *16*, 436–468, doi:10.1111/j.2153-3490.1964.tb00181.x.
Evaristo, J., S. Jasechko, and J. J. McDonnell (2015), Global separation of plant transpiration from groundwater and streamflow, *Nature*, *525*(7567), 91–94, doi:10.1038/nature14983.

Food and Agriculture Organization of the United Nations (2015), Disaster risk programme to strengthen resilience in the Dry Corridor in Central America. [Available at http://www.fao.org/resilience/resources/resources-detail/en/c/330164/, accessed on March 24th, 2016.]

Foster, S., and A. MacDonald (2014), The 'water security' dialogue: Why it needs to be better informed about groundwater, *Hydrogeol. J.*, *22*(7), 1489–1492, doi:10.1007/s10040-014-1157-6.

Franke, R. (1982), Smooth interpolation of scattered data by local thin plate splines, *Comput. Math. Appl.*, *8*(4), 273–281, doi:10.1016/0898-1221(82)90009-8.

Genereux, D. P., and M. Jordan (2006), Interbasin groundwater flow and groundwater interaction with surface water in a lowland rainforest, Costa Rica: A review, *J. Hydrol.*, *320*(3), 385–399, doi:10.1016/j.jhydrol.2005.07.023.

Giordano, M., and T. Shah (2014), From IWRM back to integrated water resources management, *Int. J. Water Resour. Dev.*, *30*(3), 364–376, doi:10.1080/07900627.2013.851521.

Giorgi, F. (2006), Climate change hot-spots, *Geophys. Res. Lett.*, *33*, L08707, doi:10.1029/2006GL025734.

Good, S. P., Mallia, D. V., Lin, J. C., and Bowen, G. J. (2014), Stable isotope analysis of precipitation samples obtained via crowdsourcing reveals the spatiotemporal evolution of superstorm Sandy, *PLoS One*, *9*(3), e91117, doi:10.1371/journal.pone.0091117.

Good, S. P., D. Noone, N. Kurita, M. Benetti, and G. J. Bowen (2015), D/H isotope ratios in the global hydrologic cycle, *Geophys. Res. Lett.*, *42*, 5042–5050, doi:10.1002/2015GL064117.

Gröning, M., H. O. Lutz, Z. Roller-Lutz, M. Kralik, L. Gourcy, and L. Pöltenstein (2012), A simple rain collector preventing water re-evaporation dedicated for δ 18 O and δ 2 H analysis of cumulative precipitation samples, *J. Hydrol.*, *448*, 195–200, doi:10.1016/j.jhydrol.2012.04.041.

Gupta, P., D. Noone, J. Galewsky, C. Sweeney, and B. H. Vaughn (2009), Demonstration of high-precision continuous measurements of water vapor isotopologues in laboratory and remote field deployments using wavelength-scanned cavity ring-down spectroscopy (WS-CRDS) technology, *Rapid Commun. Mass. Spectrom.*, *23*(16), 2534–2542, doi:10.1002/rcm.4100.

Heilweil, V. M., D. K. Solomon, S. B. Gingerich, and I. M. Verstraeten (2009), Oxygen, hydrogen, and helium isotopes for investigating groundwater systems of the Cape Verde Islands, West Africa, *Hydrogeol. J.*, *17*(5), 1157–1174, doi:10.1007/s10040-009-0434-2.

International Atomic Energy Agency/World Meteorological Organization (2015), Global network of isotopes in precipitation and global network of isotopes in river, The GNIP and GNIR Databases. [Available at http://www.iaea.org/water, accessed on 21, December, 2015.]

International Atomic Energy Agency (IAEA) (2012), Technical procedures for GNIP stations, Vienna, Austria, p. 12. [Available at http://www-naweb.iaea.org/napc/ih/documents/other/gnip_manual_v2.02_en_hq.pdf, accessed on January 26, 2016.]

Jasechko, S., and Taylor, R. G. (2015), Intensive rainfall recharges tropical groundwaters, *Environ. Res. Lett.*, *10*(12), 124015, doi:10.1088/1748-9326/10/12/124015.

Jasechko, S., Z. D. Sharp, J. J. Gibson, S. J. Birks, Y. Yi, and P. J. Fawcett (2013), Terrestrial water fluxes dominated by transpiration, *Nature*, *496*(7445), 347–350, doi:10.1038/nature11983.

Kendall, C., and T. B. Coplen (2001), Distribution of oxygen-18 and deuterium in river waters across the United States, *Hydrol. Process.*, *15*(7), 1363–1393, doi:10.1002/hyp.217.

Knutson, T. R., T. L. Delworth, K. W. Dixon, I. M. Held, J. Lu, V. Ramaswamy, M. D. Schwarzkopf, G. Stenchikov, and R. J. Stouffer (2006), Assessment of twentieth–century regional surface temperature trends using the GFDL CM2 coupled models, *J. Climate*, *19*, 1624–1651, doi:10.1175/JCLI3709.1.

Lachniet, M. (2009), Climatic and environmental controls on speleothem oxygen-isotope values, *Quaternary Sci. Rev.*, *28*(5–6), 412–432, doi:10.1016/j.quascirev.2008.10.021.

Lachniet, M., and W. Paterson (2009), Oxygen isotope values of precipitation and surface waters in northern Central America (Belize and Guatemala) are dominated by temperature and amount effects, *Earth Planet. Sci. Lett.*, *284*, 435–446, doi:10.1016/j.epsl.2009.05.010.

Lachniet, M. S., Patterson, W. P., Burns, S., Asmerom, Y., and Polyak, V. (2007), Caribbean and Pacific moisture sources on the Isthmus of Panama revealed from stalagmite and surface water δ18O gradients, *Geophys. Res. Lett.*, *34*, L01708, doi:10.1029/2006GL028469.

LeGrande, A. N., and G. A. Schmidt (2006), Global gridded data set of the oxygen isotopic composition in seawater. *Geophys. Res. Lett.*, *33*, L12604, doi:10.1029/2006GL026011.

Leibundgut, C., P. Maloszewski, and C. Kulls (2009), *Tracers in Hydrology*, 415 pp., Wiley-Blackwell, Oxford.

Magaña, V., J. A. Amador, and S. Medina (1999), The midsummer drought over Mexico and Central America, *J. Climate*, *12*(1967), 1577–1588, doi:10.1175/1520-0442(1999)012<1577:TMDOMA>2.0.CO;2.

Maldonado, T., E. Alfaro, B. Fallas-López, and L. Alvarado (2013), Seasonal prediction of extreme precipitation events and frequency of rainy days over Costa Rica, Central America, using Canonical Correlation Analysis, *Adv. Geosci.*, *33*(33), 41–52, doi:10.5194/adgeo-33-41-2013.

McDonnell, R. (2008), Challenges for integrated water resources management: How Do we provide the knowledge to support truly integrated thinking?, *Int. J. Water Resour. Dev.*, *24*(1), 131–143, doi:10.1080/07900620701723240.

Moderate Resolution Imaging Spectroradiometer (2014), Global Evapotranspiration Project (MOD16) from the Numerical terradynamic simulation group, Univ. of Montana. [Available at http://www.ntsg.umt.edu/project/mod16, accessed on January 26, 2016.]

Moerman, J. W., K. M. Cobb, J. F. Adkins, H. Sodemann, B. Clark, and A. Tuen (2013), Diurnal to interannual rainfall δ^{18}O variations in northern Borneo driven by regional hydrology, *Earth Planet. Sci. Lett.*, *369–370*, 108–119, doi:10.1016/j.epsl.2013.03.014.

Moerman, J. W., K. M. Cobb, J. W. Partin, A. N. Meckler, S. A. Carolin, J. F. Adkins, S. Lejau, J. Malang, B. Clark, and A. A. Tuen (2014), Transformation of ENSO-related rainwater to dripwater δ18O variability by vadose water mixing, *Geophys. Res. Lett.*, *41*, 7907–7915, doi:10.1002/2014GL061696.

Mook, W. G. (2006), *Introduction to Isotope Hydrology*, 223 pp., Taylor and Francis, London, U. K.

Munksgaard, N. C., Zwart, C., Kurita, N., Bass, A., Nott, J., and Bird, M. I. (2015), Stable isotope anatomy of tropical cyclone Ita, North-Eastern Australia, April 2014, *PLoS One*, *10*(3), e0119728, doi:10.1371/journal.pone.0119728.

Peña-Arancibia, J. L., A. I. J. M. van Dijk, M. Mulligen, and L. A. Bruijzeel (2010), The role of climatic and terrain attributes in estimating baseflow recession in tropical catchments, *Hydrol. Earth Syst. Sci.*, *7*, 4059–4087, doi:10.5194/hess-14-2193-2010.

Risi, C., Bony, S., Vimeux, F., and Jouzel, J. (2010), Water-stable isotopes in the LMDZ4 general circulation model: Model evaluation for present-day and past climates and applications to climatic interpretations of tropical isotopic records, *J. Geophys. Res.*, *115*, D12118, doi:10.1029/2009JD013255.

Sáenz, F., and A. M. Durán-Quesada (2015), A climatology of low level wind regimes over Central America using weather type classification approach, *Front. Earth Sci.*, *3*(15), 1–18, doi:10.3389/feart.2015.00015.

Salguero-Arias, M. E., M. Losilla-Peñón, and S. Arredondo-Li (2006), Estado del conocimiento del agua subterránea en Costa Rica, *Bol. Geol. Min.*, *117*(1), 63–73.

Sánchez-Murillo, R., G. Esquivel-Hernández, K. Welsh, E. S. Brooks, J. Boll, R. Alfaro-Solís, and J. Valdés-González (2013), Spatial and temporal variation of stable isotopes in precipitation across Costa Rica: An analysis of historic GNIP records, *Open J. Modern Hydrol.*, *3*(4), 226–240, doi:10.4236/ojmh.2013.34027.

Sánchez-Murillo, R., et al. (2016), Key drivers controlling stable isotope variations in daily precipitation of Costa Rica: Caribbean Sea versus Eastern Pacific Ocean moisture sources, *Quaternary Sci. Rev.*, *131*(Part B), 250–261, doi:10.1016/j.quascirev.2015.08.028.

Shao, J. (1993), Linear model selection by cross-validation, *J. Am. Stat. Assoc.*, *88*(422), 486–494, doi:10.1080/01621459.1993.10476299.

Sheffield, J., and E. F. Wood (2008), Projected changes in drought occurrence under future global warming from multi-model, multi-scenario, IPCC AR4 simulations, *Clim. Dyn.*, *31*(1), 79–105, doi:10.1007/s00382-007-0340-z.

Sophocleous, M. (2002), Interactions between groundwater and surface water: The state of science, *Hydrogeol. J.*, *10*, 52–67, doi:10.1007/s10040-002-0204-x.

Taylor, P. G., W. R. Wieder, S. Weintraub, S. Cohen, C. C. Cleveland, and A. R. Townsend (2015), Organic forms dominate hydrologic nitrogen export from a lowland tropical watershed, *Ecology*, *96*, 1229–1241, doi:10.1890/13-1418.1.

Terzer, S., L. I. Wassenaar, L. J. Araguás-Araguás, and P. K. Aggarwal (2013), Global isoscapes for δ18O and δ2H in precipitation: Improved prediction using regionalized climatic regression models, *Hydrol. Earth. Syst. Sci.*, *17*(11), 4713–4728, doi:10.5194/hess-17-4713-2013.

Vimeux, F., R. Gallaire, S. Bony, G. Hoffmann, and J. C. H. Chiang (2005), What are the climate controls on dD in precipitation in the Zongo Valley (Bolivia)? Implications for the Illimani ice core interpretation, *Earth Planet. Sci. Lett.*, *240*, 205–220, doi:10.1016/j.epsl.2005.09.031.

Vrba, J., and A. Richts (2015), The global map of groundwater vulnerability to floods and droughts, Explanatory notes, International Hydrological Programme. UNESCO, Paris, France. [Available at http://unesdoc.unesco.org/images/0023/002324/232431e.pdf, accessed on March 24th, 2016.]

Vrba, J., and F. G. Renaud (2015), Overview of groundwater for emergency use and human security, *Hydrogeol. J.*, *24*, 273–276, doi:10.1007/s10040-015-1355-x.

Wassenaar, L. I., S. L. Van Wilgenburg, K. Larson, and K. A. Hobson (2009), A groundwater isoscape (δD, δ18O) for Mexico, *J. Geochem. Explor.*, *102*(3), 123–136, doi:10.1016/j.gexplo.2009.01.001.

Waylen, P. R., C. N. Caviedes, and M. E. Quesada (1996), Interannual variability of monthly precipitation in Costa Rica, *J. Clim.*, *9*, 2606–2613, doi:10.1175/1520-0442(1996)009<2606:IVOMPI>2.0.CO;2.

West, A. G., E. C. February, and G. J. Bowen (2014), Spatial analysis of hydrogen and oxygen stable isotopes ("isoscapes") in ground water and tap water across South Africa, *J. Geochem. Explor.*, *145*, 213–222, doi:10.1016/j.gexplo.2014.06.009.

Yamanaka, T., Y. Makino, Y. Wakiyama, K. Kishi, K. Maruyama, M. Kano, W. Ma, and K. Suzuki (2015), How reliable are modeled precipitation isoscapes over a high-relief mountainous region?, *Hydrol. Res. Lett.*, *9*(4), 118–124, doi:10.3178/hrl.9.118.